

Spatially selective disordering of InGaAs/GaAs quantum wells using an AIAs native oxide and thermal annealing technique

Chao-Kun Lin, Xingang Zhang, P. Daniel Dapkus, and Daniel H. Rich

Departments of Electrical Engineering/ElectroPhysics and Materials Science and Engineering, University of Southern California, Los Angeles, California 90089

(Received 13 June 1997; accepted for publication 26 September 1997)

An InGaAs/GaAs quantum well (QW) disordering technique using AIAs native oxide and thermal annealing is presented. Unlike dielectric cap disordering, the AIAs native oxide can be placed close to quantum wells allowing for a spatially selective disordering deep within multilayer structures. The QW energy shifts and spatial control of the disordering were studied with photoluminescence and cathodoluminescence. The QW energy shift of thermally disordered regions containing buried oxide layer is ~ 45 meV greater than that of regions not containing buried oxide layers. The disordering transition width is estimated to be ~ 1 μm . © 1997 American Institute of Physics. [S0003-6951(97)03047-7]

A spatially selective modification of the quantum well absorption edge is necessary for certain types of integrated photonic devices, such as low loss interconnects, extended cavity lasers, phase modulators, and distributed Bragg reflectors. These devices all require the quantum well (QW) in the passive waveguide sections to be transparent at the operating wavelength to reduce the absorption loss. A number of QW disordering techniques, such as impurity-induced layer disordering,¹ ion-implantation-enhanced disordering,^{2,3} and impurity-free vacancy diffusion (IFVD),⁴⁻⁸ have been developed for this purpose and successfully applied to the monolithic fabrication of integrated optoelectronics devices and low loss wave guides. Among all of these disordering methods, IFVD is considered to be the most promising technique because no impurity is introduced into the active region of devices, thus preserving the electrical properties and crystal quality of the devices. Usually, IFVD is accomplished by depositing a thin dielectric cap layer of SiO_2 on the surface of a sample followed by thermal annealing to promote Ga atom out-diffusion into the SiO_2 cap. The Ga vacancies from the surface diffuse into GaAs/AlGaAs QW and enhance Al-Ga atom interdiffusion between the well and barriers to alter the QW energy gap. IFVD can be masked with SiN_x , and only the QW under SiO_2 is disordered. Planar buried heterostructure lasers have been fabricated using this technique. The localized change in electrical and optical properties of QWs can provide lateral confinement for both carriers and optical fields thus improving the performance of lasers.

Recently, the discovery of selective wet oxidation of high Al content AlGaAs alloys⁹ has had a great impact in the field of optoelectronics. The use of AIAs native oxide current apertures in vertical cavity surface emitting lasers (VCSELs) significantly improves the device performance. The threshold current decreases linearly as the current aperture size scales down. However, the threshold current reaches a minimum when the current aperture size is about 2 $\mu\text{m} \times 2$ μm , and further reduction of the aperture size does not decrease the threshold current.¹⁰ In fact, the native oxide current aperture only funnels the carriers into a small area of the active region. The carriers tend to diffuse laterally in the active region after they pass through the aperture and those carriers outside

the pumping region contribute no gain to the laser operation. When the size of the current aperture is comparable to the carrier diffusion length, the amount of carriers outside the pumping area cannot be ignored. As a result, the threshold current increases dramatically for those small aperture devices. Therefore, a certain kind of lateral confinement structure for carriers in the active region is necessary to further reduce thresholds.

The energy shift of disordered QWs not only depends on the annealing temperature, dielectric cap thicknesses but also the distance between the quantum well and the surface.^{6,8} The typical thickness of a VCSEL's top DBR is about 3–5 μm . It's difficult to construct a lateral confinement structure in VCSELs with traditional IFVD, although high spatial selectivity of IFVD for thin epi structures has been demonstrated.^{6,7} An alternate QW disordering technique is desirable.

Various kinds of dielectric cap materials have been studied for their effect on QW disordering.^{8,11} The concentration of oxygen in the encapsulating film greatly affects the degree of Ga atom out-diffusion into the dielectric film after heat treatment.¹¹ Native oxide current apertures used in VCSELs contain oxygen and can therefore be placed very close to the QWs making them good candidates as a point defect and/or strain source to promote QW disordering and the attendant QW energy shifts.

Strained InGaAs/GaAs QWs have been used in many device applications because of the strain modification of the band structure that leads to low threshold laser operation and high mobility carrier transport. Since In atoms are more mobile than Ga and Al atoms, a stronger QW disordering effect is expected in InGaAs/GaAs QWs¹²⁻¹⁷ compared to the GaAs/AlGaAs QWs. In this letter, the QW disordering effect in InGaAs/GaAs QWs using a buried AIAs native oxide and thermal annealing is demonstrated for the first time.

The structures, shown in Fig. 1, used in this study were grown by metalorganic chemical vapor deposition (MOCVD) on Si-doped n^+ (100) GaAs substrate, and all the layers were undoped. A 50-Å-thick $\text{In}_{0.27}\text{Ga}_{0.73}\text{As}$ QW with 150-Å-thick GaAs barriers were embedded in 1000 Å $\text{Al}_{0.2}\text{Ga}_{0.8}\text{As}$ cladding layers. The thickness of AIAs layer is

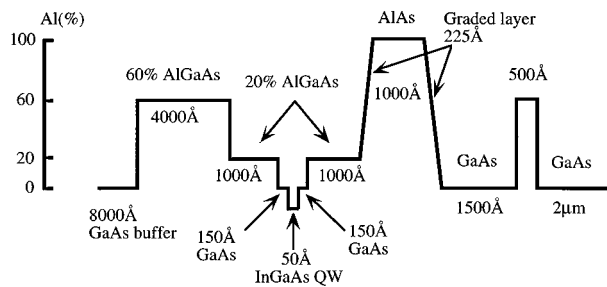


FIG. 1. A schematic of the QW structure used in this study.

1000 Å. The graded layers on both sides of AlAs layer are designed to relieve the thermal stress between oxide and semiconductor when the samples undergo the subsequent heat treatment. A 2 μm GaAs cap layer is used to prevent the surface defects (vacancies) from diffusing into the quantum well¹⁸ that could also cause QW disordering and affect the experimental results. The 500 Å Al_{0.6}Ga_{0.4}As etch stop layer prevents over etching at the GaAs cap removal step.

To examine the effect of QW disordering by using a native oxide, the samples were patterned into 500-μm-wide stripe mesas with 50 μm separations using conventional photolithography and wet chemical etching. The samples were etched all the way down to GaAs buffer layer and the AlAs layer edges were exposed for wet oxidation. The wet oxidation of the AlAs was carried out in a 425 °C open quartz tube furnace with 300 sccm ultrahigh purity N₂ bubbled through an 88 °C D.I. water bubbler. After oxidation, Al_xO_y layers, about 70 μm wide, were formed laterally on both sides of the mesas. These samples were heated to various temperatures in a rapid thermal annealer with a flowing nitrogen atmosphere. The samples were placed face down on a GaAs substrate and sandwiched by another wafer to prevent As desorption from the surface. The temperature ramping rate was 1 °C/s, sufficiently slow so as to avoid cracking of the oxide. The temperature of the sample was held at the steady state temperature for 30 s, for each heating cycle.

After the removal of the 2 μm GaAs cap layer, the samples were examined by both photoluminescence (PL) and cathodoluminescence (CL) at room temperature and low temperature, respectively, to determine the change in the emission wavelength of the QWs and the spatial control of the disordering. The CL measurements were performed with a modified JEOL 840-A scanning electron microscope. The light was detected with a liquid nitrogen cooled Ge detector. An electron beam with energy of 15 keV and current of 2 nA was used to probe the samples. During the CL measurements, the samples were maintained at 87 K.

Figure 2 illustrates the room-temperature PL emission energy of the InGaAs/GaAs QW for the disordered samples in the oxidized and unoxidized portions. The energy shift was measured with respect to the QW energy of the unannealed sample. A significant blue-shift is evident in the AlAs native oxide region. The interdiffusion between the QW and the barriers is more clearly enhanced by the presence of native oxide layers. The energy shift reaches 63.6 meV at a 900 °C annealing temperature. This result is comparable to that achieved with conventional IFVD using a SiO₂ cap. Intrinsic intermixing of the InGaAs/GaAs quantum wells was

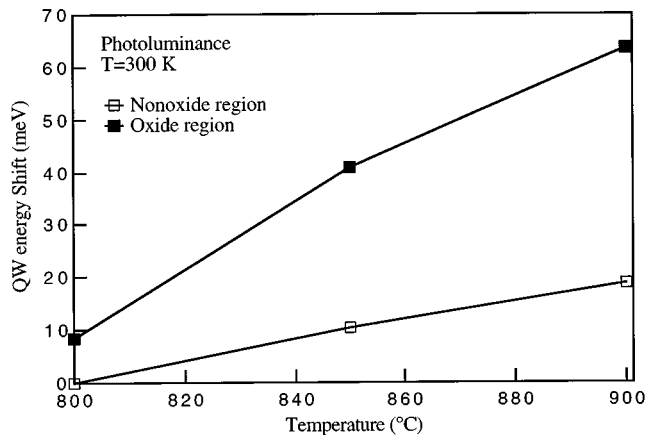


FIG. 2. Room-temperature PL measurement of QW emission in both oxide and nonoxide regions. For various end-point annealing temperatures, the energy shifts were measured with respect to the PL peak wavelength of as-grown sample (986 nm).

non-negligible when the annealing temperature exceeded 800 °C. In comparison, the intrinsic interdiffusion of GaAs/AlGaAs system is not significant until the annealing temperature over 950 °C.⁷ The maximum relative energy difference between oxide and nonoxide region is 44.8 meV, which is reduced by the intrinsic intermixing at the nonoxide region. The annealing time is actually more than 30 min, owing to the slow temperature ramping rate of 1 °C/s. Disorder effects will likely occur during the temperature ramping stages in the high-temperature regime, thus the annealing time and temperature dependence of the QW disordering effect is not easy to determine.

The spatial selectivity and control of this technique is an important consideration for fabricating confinement structures. To investigate the sharpness of the transition of QW emission at the boundary of oxide/nonoxide region, spatially resolved CL is employed owing to its high spatial resolution. The low-temperature (87 K) CL results, shown in Fig. 3(a), illustrate the variation of the normalized CL spectrum across the oxide/nonoxide region boundary. There is only one low-energy QW emission peak observed within the area that contains no oxide (distance > 0). This peak we attribute to the as-grown quantum well that may be slightly disordered by thermally driven disordering. However, two peaks are observed as the electron beam moves into the oxide region (distance < 0). The low-energy peak is again attributed to emission originating from the as-grown (nondisordered) quantum well regions outside the oxide region. This emission persists when the electron beam is well into the region with the oxide, presumably because carriers generated in the oxide disordered region diffuse to the order/disorder boundary and are swept by the band-gap gradient into the nondisordered region with smaller band gap. The high energy peak is attributed to emission originating from disordered QW regions under the oxide. In Fig. 3(b), the QW emission peak intensity ratio ($I_{\text{oxide}}/I_{\text{nonoxide}}$) of high-energy emission originating from the oxide disordered region to the low-energy component originating from the region with no oxide, and the total CL intensity ($I_{\text{oxide}} + I_{\text{nonoxide}}$) as a function of distance to the boundary are shown. The ratio $I_{\text{oxide}}/I_{\text{nonoxide}}$ changes rapidly at the boundary, indicating that the transition

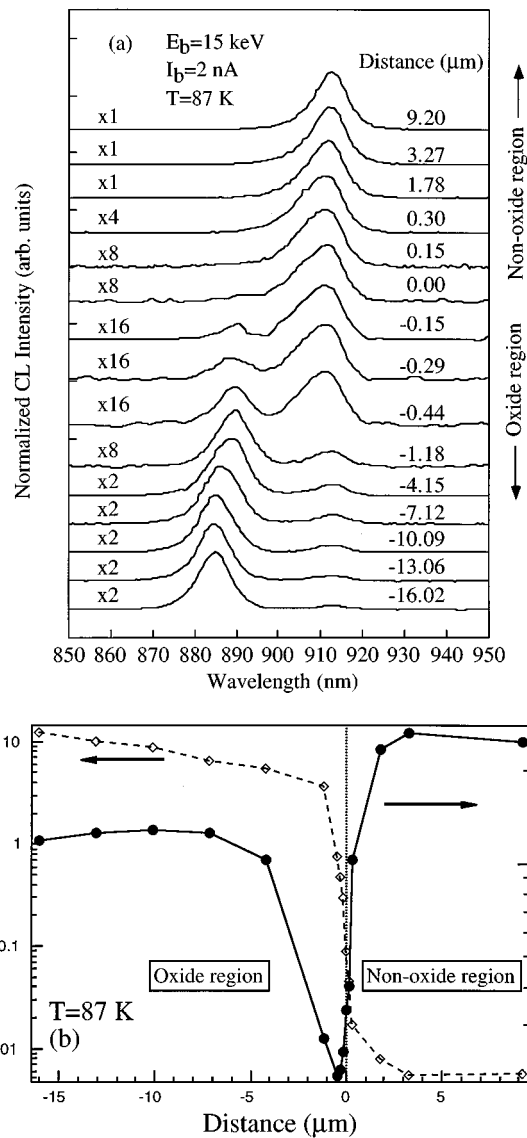


FIG. 3. Low-temperature (87 K) CL spectra of QW emission taken across the oxide/nonoxide boundary (distance=0). (a) shows a series of normalized CL spectra for various electron beam positions. The oxide region is in the negative direction and the nonoxide region is in the positive direction. (b) illustrates the CL intensity variation near the transition region. The solid line is the integrated CL intensity of both high-energy and low-energy peaks ($I_{\text{oxide}} + I_{\text{nonoxide}}$). The dashed line represents the CL peak intensity ratio between high- and low-energy peaks ($I_{\text{oxide}}/I_{\text{nonoxide}}$). The ratio changed very rapidly within $1 \mu\text{m}$ near the boundary.

region between the oxidized and nonoxidized QW is $\sim 1 \mu\text{m}$ wide. The total integrated intensity, labeled as ($I_{\text{oxide}} + I_{\text{nonoxide}}$) in Fig. 3(b), reveals that the QW emission in the oxide region is reduced relative to that in the nonoxide region by a factor of ~ 2 far away from the interface. This reduction in emission has two likely origins. First, the presence of the oxide could impede the vertical diffusive transport of carriers generated above the oxide layer to the QW (see Fig. 1). Second, the dielectric nature and lower refractive index of the oxide layer will enhance the reflection of light emitted from the QW, thereby reducing the absolute QW emission detected.

The integrated CL emission is further reduced by a factor of ~ 16 near the boundary between the oxide and nonoxide region (distance=0). The spatial variation in the disor-

dering close to this boundary causes a gradient in the effective QW band gap which will cause carriers generated near the boundary to drift toward the nonoxide (lower QW band gap) region. The built-in field will create partially a "dead region" near the boundary, markedly reducing the total radiative recombination rate. This field is also evidently responsible for the asymmetrical slope of $I_{\text{oxide}}/I_{\text{nonoxide}}$ with respect to the boundary in Fig. 3(b), as the enhanced drift of carriers in the QW from the oxide region to the nonoxide region results in the persistence of the nondisordered QW emission. This occurs for electron beam distances out to $\sim -13 \mu\text{m}$, well beyond the $\sim 1 \mu\text{m}$ carrier diffusion length.

In conclusion, we demonstrate that an InGaAs/GaAs QW's disordering effect can be induced using a buried AlAs native oxide and thermal annealing. The relative QW emission energy difference between oxide and nonoxide region is as much as 44.8 meV with a 900°C annealing temperature. The spatial selectivity and control has also been studied using spatial resolved CL. The sharp transition of CL emission at the oxide/nonoxide boundary indicates the usefulness of this technique toward forming lateral confinement structures for optoelectronics devices. Since the AlAs layer can be placed within a multilayer structure, such as the current constriction layer in a VCSEL structure, the quantum wells can be effectively disordered independent of the distance between QW and the sample surface.

This work was supported in part by an ONR grant administered by Y. S. Park.

- ¹W. D. Laidig, N. Holonyak, Jr., M. D. Carmas, K. Hess, J. J. Coleman, P. D. Dapkus, and J. Bardeen, *Appl. Phys. Lett.* **38**, 776 (1981).
- ²Y. Hirayama, Y. Suzuki, and H. Okamoto, *Jpn. J. Appl. Phys., Part 1* **24**, 1498 (1985).
- ³J. Ciber, P. M. Petroff, D. J. Weder, S. J. Pearton, A. C. Gossard, and E. English, *Appl. Phys. Lett.* **49**, 223 (1986).
- ⁴D. G. Deppe, L. J. Guido, N. Holonyak, Jr., K. C. Hsieh, R. D. Burnham, R. L. Thornton, and T. L. Paoli, *Appl. Phys. Lett.* **49**, 510 (1986).
- ⁵J. D. Ralston, S. O'Brien, G. W. Wicks, and L. F. Eastman, *Appl. Phys. Lett.* **52**, 1511 (1988).
- ⁶E. S. Koteles, B. Elman, R. P. Holmstrom, P. Melman, J. Y. Chi, X. Wen, J. Powers, D. Owens, S. Charbonneau, and M. L. W. Thewalt, *Superlattices Microstruct.* **5**, 321 (1989).
- ⁷J. Y. Chi, X. Wen, E. S. Koteles, and B. Elman, *Appl. Phys. Lett.* **55**, 855 (1989).
- ⁸J. Beauvais, J. H. Marsh, A. H. Kean, A. C. Bryce, and C. Button, *Electron. Lett.* **28**, 1671 (1992).
- ⁹J. M. Dalesasse, N. Holonyak, Jr., A. R. Sugg, T. A. Richard, and N. Elzein, *Appl. Phys. Lett.* **57**, 2844 (1990).
- ¹⁰Y. Cheng, Ph.D. dissertation, University of Southern California, 1997.
- ¹¹M. Kuzuhara, T. Nozaki, and T. Kamejima, *J. Appl. Phys.* **66**, 5833 (1989).
- ¹²J. Y. Chi, Emil S. Koteles, and R. P. Holmstrom, *Appl. Phys. Lett.* **53**, 2185 (1988).
- ¹³T. Miyazawa, Y. Suzuki, Y. Kawamura, H. Asai, and O. Mikami, *Jpn. J. Appl. Phys., Part 2* **28**, L730 (1989).
- ¹⁴S. O'Brien, J. R. Shealy, D. P. Bour, L. Elbaum, and J. Y. Chi, *Appl. Phys. Lett.* **56**, 1365 (1990).
- ¹⁵S. Sudo, H. Onishi, Y. Nakano, Y. Shimogaki, K. Tada, M. J. Mondry, and L. A. Coldren, *Jpn. J. Appl. Phys., Part 1* **35**, 1276 (1996).
- ¹⁶J. S. Tsang, C. P. Lee, S. H. Lee, K. L. Tsai, C. M. Tsai, and J. C. Fan, *J. Appl. Phys.* **79**, 664 (1996).
- ¹⁷K. Rammohan, D. H. Rich, M. H. MacDougal, and P. D. Dapkus, *Appl. Phys. Lett.* **70**, 1599 (1997).
- ¹⁸L. J. Guido, N. Holonyak, Jr., K. C. Hsieh, and J. E. Baker, *Appl. Phys. Lett.* **54**, 262 (1989).